Impacts of Synoptic Patterns and Meteorological Factors on Distribution Trends of Ozone in Southeast China During 2015–2020

Xiaoting Ji[1,2,3], Youwei Hong[1,2,3,4] (ID), Yiling Lin[1,2,5], Ke Xu[1,2,4], Gaojie Chen[1,2,3], Taotao Liu[1,2,3], Lingling Xu[1,2,3], Mengren Li[1,2], Xiaolong Fan[1,2], Hong Wang[6], Hongliang Zhang[7], Yuping Chen[1,2,3], Chen Yang[1,2,3], Ziyi Lin[1,2,3], and Jinsheng Chen[1,2,3] (ID)

[1]Center for Excellence in Regional Atmospheric Environment, Institute of Urban Environment, Chinese Academy of Sciences, Xiamen, China, [2]Key Lab of Urban Environment and Health, Institute of Urban Environment, Chinese Academy of Sciences, Xiamen, China, [3]University of Chinese Academy of Sciences, Beijing, China, [4]School of Life Sciences, Hebei University, Baoding, China, [5]College of Chemical Engineering, Huaqiao University, Xiamen, China, [6]Fujian Key Laboratory of Severe Weather, Fujian Meteorological Science Institute, Fuzhou, China, [7]Department of Environmental Science and Engineering, Fudan University, Shanghai, China

Abstract Surface ozone (O_3) pollution under global climate change has become one of the top environmental issues. In this study, we focused on the coastal region in Southeast China with relatively low O_3 precursor's emissions and complicated synoptic conditions, where the O_3 trends and meteorological contributions remain unclear. An increasing trend of O_3 concentrations in the cities (0.3–4.6 µg m^{-3} yr^{-1}) from 2015 to 2020 was observed. Twenty-three synoptic patterns were clustered based on weather typing method, in which cyclone-related types and southwesterly type were generally associated with low O_3 concentrations, and high O_3 levels occurred with anticyclone-related types. Considering both frequency and intensity of synoptic patterns, reconstructed O_3 series captured 46.0%–58.3% of the observed variability. Using Kolmogorov-Zurbenko filter, an increasing trend of long-term O_3 was found. By implementing the multiple linear regression model between O_3 concentrations and meteorological factors, the meteorological contributions to O_3 variabilities (44.7%–66.1%) were quantified. The results indicated the meteorological conditions were particularly important in O_3 pollution with the reductions of O_3 precursor's emissions, among which relative humidity, boundary layer height, solar radiation along with low cloud cover were proved to play important roles. The weakening southwest winds along with more anti-cyclone systems under climate change could increase surface O_3. This study elucidated the crucial meteorological drivers on the O_3 variability in relatively clean areas and implied the challenges for local governments to mitigate O_3 pollution under global climate change.

Plain Language Summary Ozone (O_3) pollution has become one of the top environmental issues in recent years and can be affected not only by O_3 precursors (volatile organic compounds and nitrogen oxides) but also meteorological condition. Under global climate change, there is a need to deeply understand the impact of meteorological factors on surface O_3 concentrations with the decrease of O_3 precursors. In this study, we focus on the coast area of Southeast China with relatively low O_3 precursors emissions and influenced by the East Asia monsoon. Temporal and spatial variations of O_3 concentrations along with the meteorological impacts on O_3 variabilities from 2015 to 2020 were analyzed. The results show that the relative meteorological contributions on O_3 trends were 44.7%–66.1%. The higher temperature, lower relative humidity, more solar radiation, weakening southwest winds along with anti-cyclone systems under climate change could increase surface O_3. This study is beneficial to understand different mechanisms of meteorological impacts on O_3 variations in the relatively clean areas, and find out the key drivers to cause O_3 pollution with the decrease of O_3 precursors emissions and climate change.

1. Introduction

Surface ozone (O_3), as an important atmospheric oxidant, is harmful to animals, vegetation growth and human health (Chang et al., 2021; Dong et al., 2020; Gao et al., 2021). In the troposphere, O_3 is produced through a series of complex photochemical oxidation of carbon monoxide and volatile organic compounds (VOC) by the hydroxyl radical (OH) under strong solar radiation (SR) and the presence of nitrogen oxides (NO$_x$) (Jing et al., 2016;

Monks et al., 2009; Shu et al., 2020). O_3 pollution level can be affected not only by O_3 precursors (VOC and NO_x) but also meteorological conditions (Jing et al., 2016; Santurtún et al., 2015; Seo et al., 2014; Yu et al., 2019). Low anthropogenic emissions of O_3 precursors by 2100 was projected in the Fifth Assessment Report of the Intergovernmental Panel on Climate Change and it suggested that climate-induced shifts in meteorology will likely offsetting the benefits of emission reductions (Schnell et al., 2016). Thus, quantitatively understanding the contributions of anthropogenic emissions and meteorological conditions to O_3 formations is of great importance for the mitigation policy of air pollution.

Meteorological factors could affect O_3 concentrations through a series of processes, including emissions, chemical reactions, transport and removal of O_3 and its precursors (Liu et al., 2019; Lu et al., 2019). Many studies have found high O_3 concentrations associated with high temperature, low relative humidity (RH), strong SR and stagnant weather (Hertig et al., 2019; Zhang et al., 2018). J. Zhang et al. (2022) found that mean warming over the contiguous United States dominates the impacts of climate change on ozone. Since local meteorological conditions are greatly determined by synoptic patterns, and synoptic classification could be a useful method to explore the impact of meteorological factors on surface O_3 concentrations. The dominant weather types and the relation between synoptic patterns and O_3 concentration varied in different regions (Chen et al., 2021; Dong et al., 2020; Gao et al., 2021; Liu et al., 2019). Mousavinezhad et al. (2021) suggested that the impact of meteorological conditions on O_3 levels could largely offset the effects of emissions change in the Beijing-Tianjin-Hebei of China. Taking into account variabilities in frequency and intensity of synoptic patterns, Liu et al. (2019) reconstructed the time series of O_3 and captured up to 39.2% of the observed interannual variability. It has been suggested that meteorological conditions could be the determining factor on O_3 formation under low levels of anthropogenic emissions (Lu et al., 2019; Wu et al., 2017).

Under global climate change with extreme weather conditions, identifying the contributions of meteorological influence to O_3 is necessary for understanding O_3 pollution. Schnell et al. (2016) found that climate change obviously increased the percentage of high daily O_3 concentration, even with constant biogenic emissions. In China, the implement of "Air Pollution Preventions and Action Plan" (2013–2017) and "Blue Sky Protection Campaign" (2018–2020) have led to the remarkable reductions of criteria air pollutants but not of O_3 (Gao et al., 2021; Lu et al., 2018; Shu et al., 2020). However, current studies were focused on surface O_3 pollution in megacities (Chang et al., 2021; Dong et al., 2020; Zhan et al., 2020), and the impacts of meteorological factors on O_3 pollution in coastal cities with relatively low O_3 precursor emissions were scarce (Wang et al., 2022). Fujian Province, located in the coastal area of Southeast China, shows lower NO_x emissions than those in other coastal provinces (Table S1 in Supporting Information S1) and is one of the provinces with good air quality in China (X. Zhang et al., 2022). Thus, this study could provide a scientific basis for meteorological influence mechanisms of O_3 pollution in other regions of China with the reduction of O_3 precursor emissions. In addition, compare to the inland cities, coastal areas were more easily affected by air masses originated from the ocean. Meanwhile, small scale circulations such as sea-land breezes could also affect O_3 levels under weak synoptic forcing (Seo et al., 2014; Wang et al., 2022). The mechanisms of meteorological impact on surface O_3 variations in inland and coastal areas could be quite different. These provided a good chance to study the contributions of meteorological conditions to O_3 formations under global climate change.

In Section 2, we described the data and analysis methods in our study. In Section 3.1, temporal and spatial variations of O_3 concentrations in the coastal area of Southeastern China from 2015 to 2020 were analyzed. In Section 3.2, weather typing was implemented to determine the dominant synoptic patterns and related local meteorological conditions, which might lead to high O_3 concentration. The contributions of synoptic patterns were quantified. In Section 3.3, local meteorological factors and circulation indexes were selected for meteorological adjustment to analyze the long-term trends of O_3 and meteorological conditions. The results were beneficial to understand different mechanisms of meteorological impacts on O_3 variations in the relatively clean areas, and find out the key drivers to cause O_3 pollution with the decrease of O_3 precursor's emissions. This study will provide a scientific basis for other region governments to control O_3 pollution with the reductions of anthropogenic emissions and climate change.

2. Materials and Methods

2.1. Ozone and Meteorological Data Sets

Fujian is located on the western side of the Taiwan Strait and affected by the long-range transport of air pollutants from the Yangtze River Delta (YRD) and the Pearl River Delta, which are the two most developed regions of
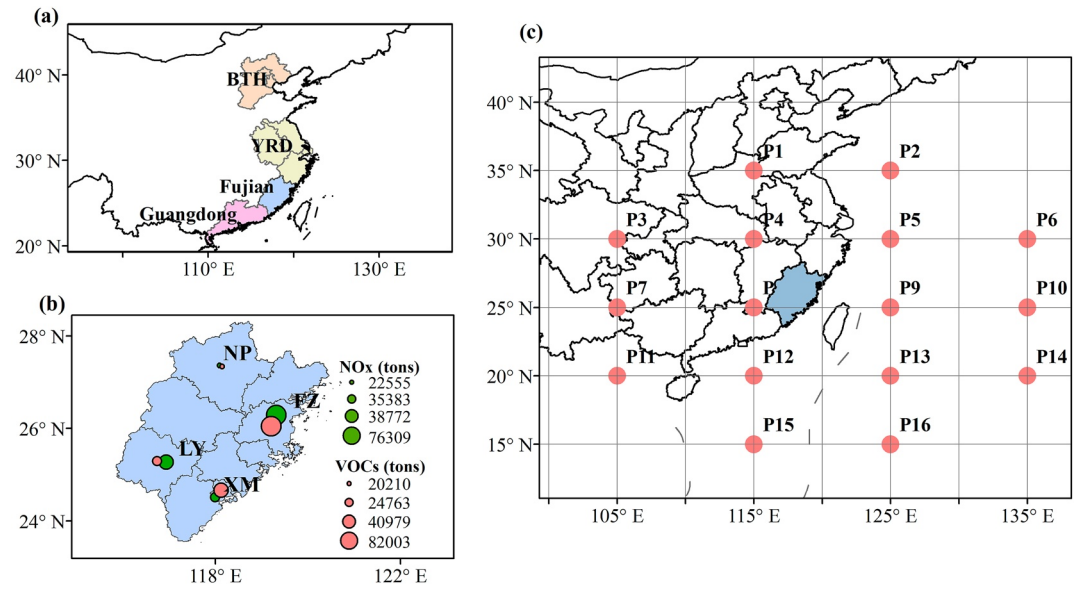
Figure 1. The locations of Fujian Province, Beijing-Tianjin-Hebei (BTH), Yangtze River Delta and Guangdong Province in China (a) and the four monitoring sites (XM, FZ, LY, and NP) in Fujian Province, the green and red dot represents the levels of O_3 precursor's emissions (b); 16 grid points used to calculate circulation indexes (c).

China (Figure 1a). In this study, four cities were chosen to represent the region for inter-annual analysis of surface O_3 concentrations. Xiamen (XM) and Fuzhou (FZ) are the two eastern coastal cities with rapid urbanization and industrialization development, while the economic development and anthropogenic activities emissions are relatively low in Longyan (LY) and Nanping (NP). The comparison of O_3 precursors (NO_x and VOCs) emissions in these cities were shown in Figure 1b and it was indicated that the air quality of NP and LY were cleaner than that of FZ and XM. The VOCs levels in the two eastern coastal cities were obviously higher than in those western mountainous cities (X. Zhang et al., 2022). The maximum daily 8 hr average (MDA8) O_3 concentrations in four cities from 2015 to 2020 were calculated, according to the Ambient Air Quality Standard of China. Hourly ground-level O_3 concentrations were monitored by the instruments of TEI 49i (Thermo Fisher Scientific, Waltham, MA, USA), and the uncertainty of O_3 measurement were ±5%.

To identify the synoptic patterns, we used mean sea level pressure (MSLP) data in 6 hr intervals (Beijing time 02:00, 08:00, 14:00, and 20:00) for 2015–2020 with a resolution of 2.5° × 2.5° from the National Centers for Environmental Prediction/National Center for Atmospheric Research (NECP/NCAR) reanalysis data (https://psl. noaa.gov/data/gridded/data.ncep.reanalysis.html, last access: 28 December 2021). The hourly data of meteorological factors including temperature at 2 m (T), RH, U and V wind components at 10 m (U_{10} and V_{10}, respectively), SR, low cloud cover (LCC), total precipitation (TP) and boundary layer height (BLH) were obtained from the fifth generation European Centre for Medium-Range Weather Forecasts reanalysis data set (ERA5) (https://www. ecmwf.int/en/forecasts/datasets/reanalysis-datasets/era5, last access: 24 March 2022).

2.2. Lamb-Jenkinson Circulation Classification

The Lamb-Jenkinson weather typing approach proposed by Lamb (1950) and developed by Jenkinson and Collison (1977) has been widely employed to classify synoptic circulation, due to the automation and explicit meteorological meaning (Jiang et al., 2021; Liu et al., 2019; Wang et al., 2017; Yan et al., 2021). To calculate the circulation types of the study area covering the four cities, 16 points (105–135°E, 15–35°N) were marked at every 10° longitudes and 5° latitude with a center located in Fujian Province (Figure 1c). The daily MSLP of 16 points were averaged over four time points to calculate six circulation indexes: southerly flow component of the geostrophic surface wind (u), westerly flow component of the geostrophic surface wind (v), resultant flow (V), southerly shear vorticity (ξ_u), westerly shear vorticity (ξ_v) and total shear vorticity (ξ). The calculation methods for each index are shown in Supporting Information S1 (Text S1). Following the rules described in Trigo and DaCamara (2000), the synoptic patterns were predefined by comparing values of ξ

and V (Table S2 in Supporting Information S1), and direction of follow is given by $\tan^{-1}(v/u)$. Each day can be determined objectively as one certain pattern. This method allows 26 different weather types to be defined with eight directional types (easterly, E; northerly, N; southerly, S; westerly, W; northeasterly, NE; southeasterly, SE; southwesterly, SW; northwesterly, NW), two geostrophic vorticity (anticyclone, A and cyclone, C) and 16 hybrid types (CN (cyclone-northerly), CNE (cyclone-northeasterly), CE (cyclone-easterly), CSE (cyclone-southeasterly), CS (cyclone-southerly), CSW (cyclone-southwesterly), CW (cyclone-westerly), CNW (cyclone-northwesterly), AN (anticyclone-northerly), ANE (anticyclone-northeasterly), AE (anticyclone-easterly), ASE (anticyclone-southeasterly), AS (anticyclone-southerly), ASW (anticyclone-southwesterly), AW (anticyclone-westerly) and ANW (anticyclone-northwesterly)). Compared with other circulation classification methods, the synoptic types obtained by the Lamb-Jenkinson weather typing approach are robust and fixed. In addition, the method provides the clear pressure fields and wind fields over the study area, which can reflect the impact of prevailing wind on O_3 transport (Liu et al., 2019). In this study, according to the similar meteorological factors and mean O_3 concentrations, the synoptic types associated with low-pressure system were merged as LP (low-pressure system, including CWS, CW, CS, CNW, CNE, CN, and CE) and AN, ANE, AE, AS, AWS, AW, and ANW were merged as HP (high-pressure system).

2.3. Meteorological Adjustment

To quantify the effect of meteorological factors on MDA8 O_3 variations, meteorological adjustment, a statistical method, was used through removing the meteorological impact on O_3 series. In the method, Kolmogorov-Zurbenko (KZ) filter (Rao & Zurbenko, 1994) is applied to separate the original O_3 series and meteorological data into different components as follows:

$$O(t) = W(t) + S(t) + e(t) \tag{1}$$

where, $O(t)$ is the original series, $W(t)$ is the short-term variation on a timescale of days, $S(t)$ is the seasonal change on a timescale of months and $e(t)$ denotes the long-term components on a timescale of years. The $KZ_{(m,n)}$ filter carries out n iterations of a moving average with a window length of m, which is defined as

$$Y_i = \frac{1}{m} \sum_{j=-k}^{k} X_{i+j} \tag{2}$$

where, $m = 2k + 1$, X_{i+j} is the original series of MDA8 O_3, and the calculated Y_i is applied as an input for the next pass until the moving average is implemented n times. Different scales of motions can be obtained by changing the number of iterations and window length (Eskridge et al., 1997; Milanchus et al., 1998). The filter periods of fewer than N days can be calculated as

$$m \times n^{\frac{1}{2}} \leq N \tag{3}$$

Rao et al. (1997) found that the actual variation of O_3 at different scales can be obtained by removing several influences when $KZ_{(15,5)}$ and $KZ_{(365,3)}$ filters are applied as follows:

$$W(t) = O(t) - KZ_{(15,5)} \tag{4}$$

$$S(t) = KZ_{(15,5)} - KZ_{(365,3)} \tag{5}$$

$$e(t) = KZ_{(365,3)} \tag{6}$$

To remove the impacts of meteorological factors on the MDA8 O_3 variations, a stepwise multiple linear regression (MLR) model was used as follows:

$$P(t) = \sum_{i=1}^{n} a_i V_i + b + r \tag{7}$$

where, $P(t)$ is the predicted MDA8 O_3, n is the number of meteorological factors, a_i is a series of regression coefficients, V_i is the meteorological variable, b is the intercept term and r is the regression residual.

Factors including RH, daily max temperature (T_{max}), u component of wind speed at 10 m (U_{10}), v component of wind speed (V_{10}), SR, LCC, TP and BLH were selected to reflect local meteorological conditions and circulation indexes including southerly flow component of the geostrophic surface wind (u), westerly flow component of the geostrophic surface wind (v) and total shear vorticity (ξ) were added to present synoptic impact. We selected the meteorological factors that best fit the model by performing a stepwise MLR between the original MDA8 O_3 series and the meteorological factors. In each iteration, each meteorological variable was added and removed individually based on the statistical significance thresholds (both entering and removing thresholds were assumed to be $p = 0.05$). V component of wind speed and BLH were removed in XM and FZ, respectively. U component and V component of wind speed were removed in NP. Then we implemented the MLR model between the baseline components ($KZ_{(15,5)}$) and the selected meteorological factors. Similar analysis was applied to the short-term components. According to Rao et al. (1997), residuals represent the meteorological impact that could be attributed to the precursor emissions.

2.4. Reconstruction of O_3 Concentration Based on Synoptic Patterns

To calculate the inter-annual variability captured by the variations in the surface circulation pattern, Comrie and Yarnal (1992) provided an algorithm to separate synoptic and non-synoptic variability in environmental data and can be expressed as:

$$\overline{\overline{O_{3m}}}(\text{fre}) = \sum_{k=1}^{23} \overline{O_{3k}} F_{km} \tag{8}$$

where, $\overline{\overline{O_{3m}}}(\text{fre})$ is the reconstructed MDA8 O_3 concentration influenced by the frequency variation in the weather types for the year m, $\overline{O_{3k}}$ represents the 6-year mean MDA8 O_3 concentration for weather type k, and F_{km} represents the occurrence frequency of weather type k for year m.

Hegarty et al., 2007 applied an improved method that could better separate the environmental and climate-related contributions to the inter-annual variations in O_3 by considering not only frequency changes but also intensity variations:

$$\overline{\overline{O_{3m}}}(\text{fre} + \text{int}) = \sum_{k=1}^{23} \left(\overline{O_{3k}} + \Delta O_{3km} \right) F_{km} \tag{9}$$

where, $\overline{\overline{O_{3m}}}(\text{fre} + \text{int})$ is the reconstructed MDA8 O_3 concentration influenced by both the frequency and intensity of the changes in weather types for year m; ΔO_{3km} is the modified difference on the fitting line that obtained through a linear fitting of the annual MDA8 O_3 concentration anomalies to the circulation intensity for weather type k in year m Liu et al. (2019) and (Gao et al., 2021) provided several factors, and the one with the strongest correlation coefficient with ΔO_3 would be selected to reconstruct O_3 concentration. In this study, domain-averaged sea level pressure (mslp), the maximum sea level pressure (max slp) and the minimum sea level pressure (min slp) were applied for correlation analysis.

3. Results and Discussion

3.1. Spatiotemporal Variations of Surface Ozone

Inter-annual variations of MDA8 O_3 concentrations in XM, FZ, LY, and NP during 2015–2020 are shown in Figure 2. The average O_3 concentration in FZ (88.1 μg m^{-3}) was the highest, followed by XM (80.5 μg m^{-3}), NP (79.4 μg m^{-3}) and LY (78.3 μg m^{-3}). The O_3 increase of 4.6 μg m^{-3} or 6.8% per year in XM was the most significant ($p < 0.05$), while the variations in LY was relatively constant (0.3 μg m^{-3} or 0.5% per year, $p > 0.1$). The Xiamen port is one of the top 10 ports in China, causing the impacts of ship emissions and port activities on surface O_3 concentrations. Meanwhile, the number of motor vehicles increased sharply in recent years, resulting in large amount of O_3 precursors (NOx and VOCs) emissions. In the four cities, the elevated O_3 concentrations from 2016 to 2018 (~24.5% per year) were observed, reaching a maximum in 2018 for FZ (98.4 μg m^{-3}), NP (85.8 μg m^{-3}), LY (82.2 μg m^{-3}) and 2019 for XM (92.2 μg m^{-3}). Annual MDA8 O_3 concentrations over 1,000 sites across China increased significantly by ~50% during 2015–2017 (Silver et al., 2018). Although O_3 levels in the study was significantly lower than that in the developed regions of China, the increasing rate of
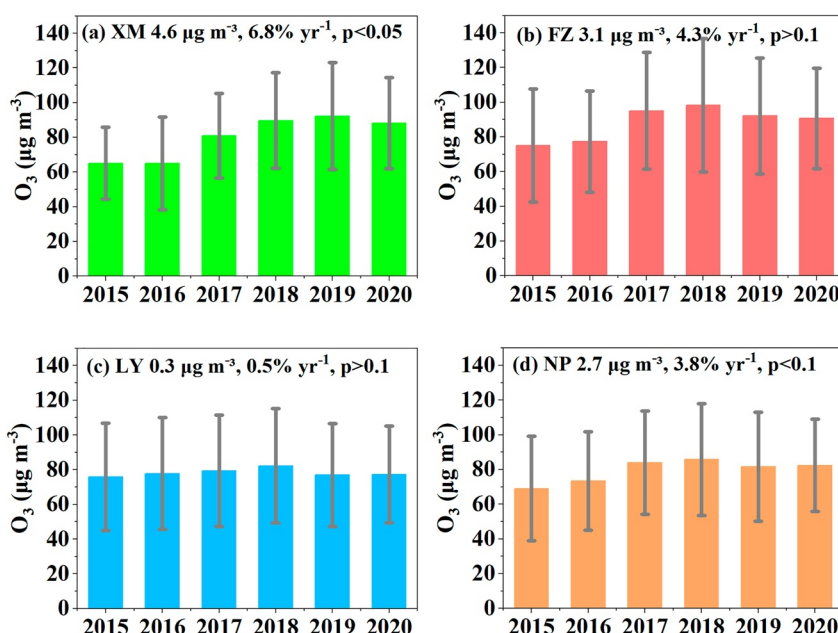
Figure 2. Inter-annual variations of MDA8 O_3 concentrations in the four cities from 2015 to 2020.

O_3 (4.6 $\mu g\ m^{-3}\ yr^{-1}$) is comparable to that in these areas, including northern China (7.88 $\mu g\ m^{-3}\ yr^{-1}$ during 2013–2017) (Liu et al., 2019), the YRD (3.86 $\mu g\ m^{-3}\ yr^{-1}$ during 2014–2018) (Gao et al., 2021) and Guangdong province (1.10 $\mu g\ m^{-3}\ yr^{-1}$ during 2014–2018) (Yin et al., 2019). Inter-annual variations of MDA8 O_3 concentrations in the four cities during 2015–2020 were mainly attributed to the impacts of meteorological conditions change, along with the decrease of PM, SO_2, and NO_x concentrations and the increase of VOCs (Wang et al., 2022).

3.2. Effect of Synoptic Patterns

3.2.1. Synoptic Pattern Classification

Based on the Lamb-Jenkinson weather typing approach, 23 synoptic patterns affecting the study area from 2015 to 2020 were clustered, including two vorticity types (cyclone, C, and anticyclone, A), 7 directional types (northerly, N; northeasterly, NE; northwesterly, NW; easterly, E; southerly, S; southwesterly, SW and westerly, W), and 14 hybrids of vorticity and directional types (CN, CNE, CE, CS, CWS, CW, CNW, AN, ANE, AE, AS, AWS, AW, and ANW). The MSLP maps are shown in Supporting Information S1 (Figure S1), and the occurrence frequency of each type is marked. The locations of the high-pressure and low-pressure centers under different weather types were obviously different. The occurrence frequencies of pure directional types, vorticity types and hybrid types were 54.3%, 18.2%, and 27.5%, respectively.

The seasonal and inter-annual exceedance ratios of 23 synoptic types are shown in Figure 3 and Table S3 in Supporting Information S1. The southeast coast of China is strongly affected by the East Asian monsoon and the key weather systems such as the western Pacific Subtropical High, the Siberian High and tropical cyclones. The predominant synoptic types are E (20.0%), C (9.7%), W (9.5%), A (8.5%) and NE (8.5%). Due to the monsoon circulation systems, the frequencies of synoptic patterns varied on a seasonal scale (Figure 3a), leading the variabilities of local meteorological conditions, which will be further discussed in Section 3.2.2. In addition, Figure 3b indicates significant inter-annual variations of synoptic patterns, which could have an effect on the long-term trend of O_3 (Gao et al., 2021; Liu et al., 2019; Zhang et al., 2013). Based on the same weather typing method, Liu et al. (2019) obtained 26 circulations patterns in northern China, where weather typing strongly affected by northern cyclones, the Siberian High and the western Pacific subtropical high, and the predominant synoptic types in the region are C (18.1%) and A (17.5%). In Guangzhou, where it has the similar meteorological condition with the study area, Liao et al. (2020) obtained 18 synoptic types and found E occurred most (38.3%). The contributions of the frequency and intensity changes of synoptic patterns on the inter-annual O_3 variability will be discussed in Section 3.2.3.
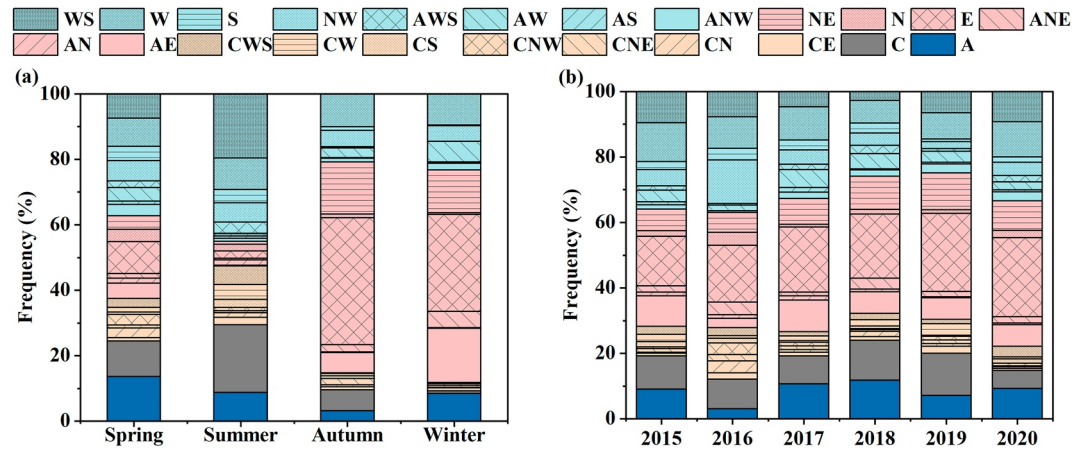
Figure 3. Seasonal (a) and inter-annual (b) frequencies of 23 weather types from 2015 to 2020. The dark blue, gray, orange, pink, and light blue areas represent the weather categories A, C, LP, HP and directional types, respectively.

3.2.2. Relationship Between Synoptic Pattern and Ozone Pollution

According to our previous study, the local meteorological conditions associated with a specific synoptic pattern could play a key role in O_3 pollution by affecting the photochemical generation and regional transport of O_3 (Liu et al., 2019). The characteristics of MDA8 O_3 concentrations and meteorological factors with 23 weather types during 2015–2020 are presented (Figure 4 and Table S4 in Supporting Information S1). Synoptic types that associated with high-pressure system (Type A and HP) were generally associated with relatively higher O_3 concentrations. As shown in Figure 3a, the frequency of type A is the highest (13.6%) in spring. Due to anticyclone control, dry weather, weak wind and strong SR were favorable to the formation and accumulation of surface O_3. Thus, the corresponding MDA8 O_3 reached 103.8 μg m^{-3} under type A. In summer, the frequencies of C (20.7%) LP (18.0%) and WS (19.6%) increased and the low O_3 concentrations were found. This was generally associated with hot, wet weather and heavy rainfall, which were favorable to the removal of O_3. These results were consisted with the fact that continuous type A contributed to high O_3 values, while type C reduced the O_3 pollution in Guangzhou (Liao et al., 2020). However, the reversed pattern was observed in the northern China (Liu et al., 2019). Under LP and C categories, there existed hot, humid air, less clouds and rainfall, which were favorable for O_3 formation and accumulation, leading the O_3 concentration peaks. The cool and dry air, moderate rain and relatively clean air masses from the Inner Mongolia or eastern ocean under type A constituted unfavorable conditions for O_3 formation in the northern China. Moreover, O_3 levels tend to be high when the prevailing wind direction was northerly wind, even under cyclone control, which could be attributed to high temperature, weak wind, strong SR and less rainfall, along with the long-distance transmission from northern cities with large emissions.

3.2.3. Quantifying the Effects of Synoptic Changes

To quantify the synoptic effects, the contribution of frequency or intensity of synoptic patterns on O_3 variabilities is defined as the difference between the maximum and minimum of the reconstructed O_3 series divided by the difference between that of the original series (Liu et al., 2019). The reconstructed inter-annual O_3 concentrations in the four cities are shown in Figure 5. Inter-annual variations of reconstructed O_3 concentrations from 2017 to 2020 in most cities are significantly reduced, compared to the observed one. However, the reverse trends from 2015 to 2016 were observed. The frequency variations in synoptic circulation in XM, FZ, LY, and NP contributed 18.7%, 18.4%, 39.4%, and 12.5% of inter-annual variability in O_3, and the contributions by frequency and intensity were 46.0%, 49.8%, 58.3%, and 42.1%, respectively, which was consisted with the fact that the rapid industrialization and urbanization in coastal area of Southeast China have been happening during the past decades. The results showed that the intensity of synoptic circulation patterns played important roles in XM, FZ, and NP, while the contribution of frequency in LY was more obvious. The contributions of frequency and intensity variations in LY was significantly higher than those in other cities, due to the slight inter-annual variations of O_3 concentrations in LY. In this study, these contributions of frequency and intensity are higher than that (36%) in Hongkong (Zhang et al., 2013). In northern China, the contributions of inter-annual variability in O_3 affected by frequency and intensity variations ranged from 44.1% to 69.8%, and the contributions by frequency-only variations ranged
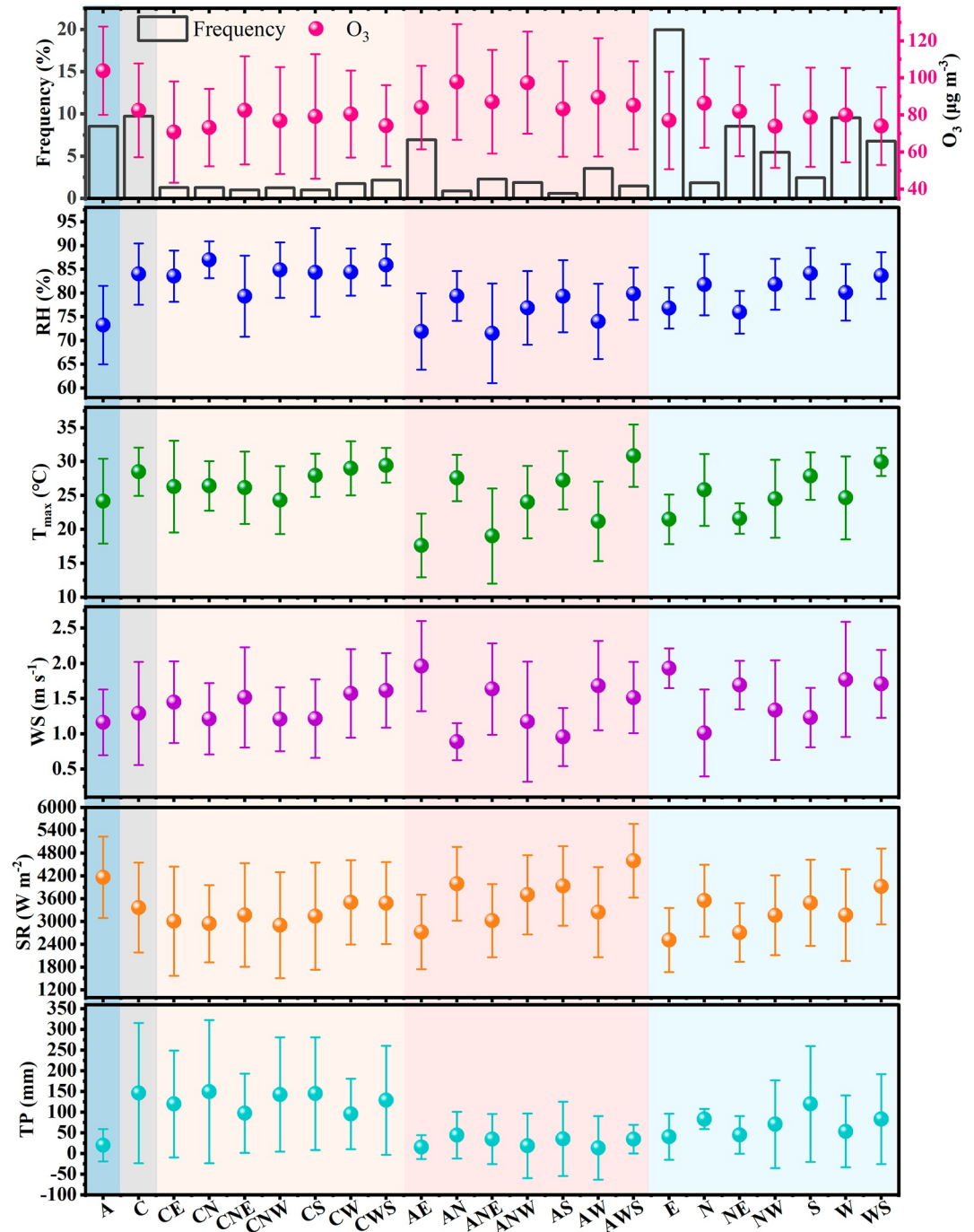
Figure 4. Mean values of MDA8 O_3 concentrations and meteorological factors in 23 weather types during 2015–2020 in the four cities. The dark blue, gray, orange, pink, and light blue areas represent the weather categories A, C, LP, HP and directional types, respectively.

from 5.2% to 23.4% (Liu et al., 2019). These results suggested that the contributions of frequency and intensity of synoptic circulation patterns were varied with the emission intensity of anthropogenic activities, and climate change played more important role in O_3 variations under relatively clean areas.
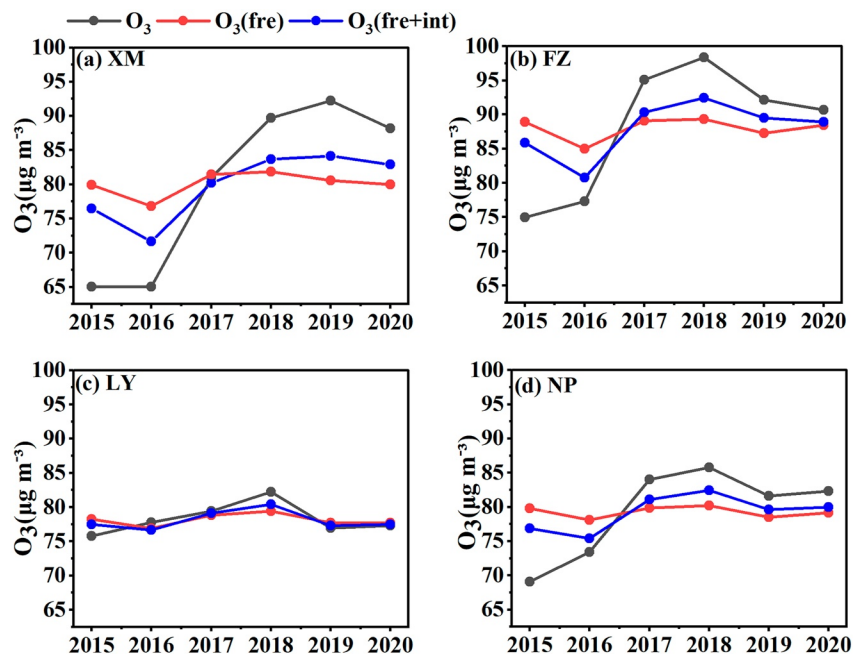
Figure 5. The inter-annual MDA8 O_3 concentration for original and reconstructed O_3 based on variations in synoptic patterns in XM(a), FZ (b), LY(c), and NP(d). The black lines represent the original inter-annual MDA8 O_3 concentrations, the red lines and blue lines represent the reconstructed O_3 concentration taking into account frequency-only and both frequency and intensity of synoptic patterns, respectively.

3.3. Effect of Meteorological Factors

3.3.1. Ozone Time Series Separated by KZ Filter

The MDA8 O_3 time series were separated using the method described in Section 2.3. The contributions of short-term, seasonal and long-term components to the total variance of the original data were shown in Table 1. The short-term components contributed the most (55.1%–67.7%) to the total variance of the original series in all four cities, which were related with synoptic-scale and mesoscale meteorological processes (Ma et al., 2016). Seasonal components (21.7%–27.5%) was the second contributor, followed by the long-term components. Quantile-quantile (Q-Q) plots of the short-term component are presented in Supporting Information S1 (Figure S2), suggesting that the short-term components were removed effectively from the original data. The long-term components have the lowest contribution to the variance of the original data, which confirmed the importance to separate the short-term and seasonal components from the original data for obtaining the long-term trend of O_3 (Ma et al., 2016; Sá

Table 1
Comparisons of Meteorological Adjustment for O_3 Variations in Coastal Cities Around the World

Site	Time range	Trend (µg cm^{-3} yr^{-1})		Meteorological contribution (%)	References
		Original O_3	Adjusted O_3		
XM	2015–2020	6.06	3.35	44.7	This study
FZ	2015–2020	3.71	1.54	58.4	This study
NP	2015–2020	2.74	0.96	65.0	This study
LY	2015–2020	0.37	−0.39	66.1	This study
BTH	2015–2019	3.36	2.29	31.8	Mousavinezhad et al. (2021)
Zhejiang	2013–2017	7.15	5.02	29.8	Yu et al. (2019)
Yangzhou	2013–2017	8.14	5.88	27.8	Yu et al. (2019)
Houston	2003–2017		1.09	51.0	Botlaguduru and Kommalapati (2020)
Portugal	2002–2012	–	–	59.0	Sá et al. (2015)
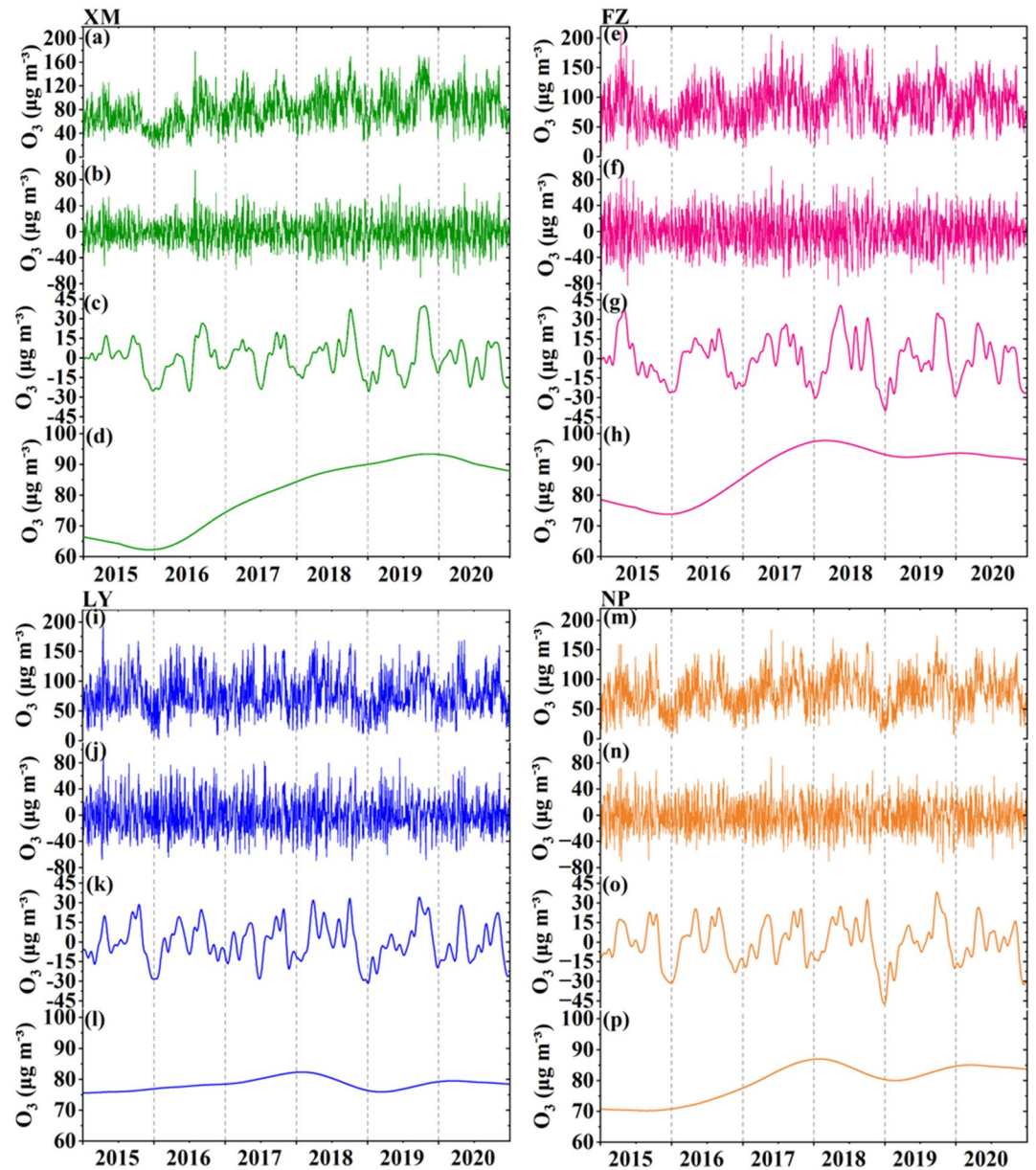
Figure 6. Separated time series of MDA8 O$_3$ in the four cities: (a), (e), (i), and (m) the original data in XM, FZ, LY, and NP, respectively; (b), (f), (j), and (n) the short-term component; (c), (g), (k), and (o) the seasonal component; (d), (h), (l), and (p) the long-term component.

et al., 2015). The percentage of long-term components (15.6%) in XM was larger than those in other cities, which was related with the impact of climate change or inter-annual fluctuation of emissions on O$_3$ variations.

Figure 6 shows the original data, short-term, seasonal and long-term component of ozone in the four cities. The original series showed obvious seasonal patterns with high frequency noises (Figures 6a, 6e, 6i, and 6m). The removal of short-term components (Figures 6b, 6f, 6j, and 6n) leads to seasonal cycles (presented in Figures 6c, 6g, 6k, and 6o). There were two peaks of O$_3$ concentrations occurred in spring and autumn, which was different with that in other regions. The O$_3$ concentrations tended to peak in summer in northern China, where strongly affected by northern cyclones, the Siberian High and the western Pacific subtropical high (Liu et al., 2019; Ma et al., 2016). As shown in Figure 3, south and southwest winds prevailed in summer and the frequencies of type C and type WS increased, due to the East Asian summer monsoon (Yang et al., 2022). The clean air mass originated from the ocean under the meteorological patterns could result in low O$_3$ concentrations due to the influence of
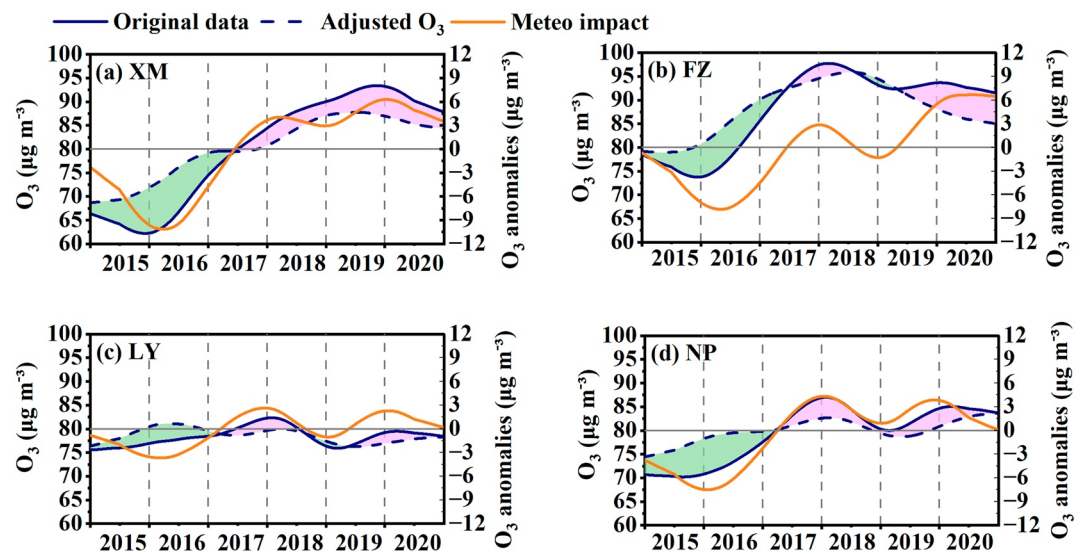
Figure 7. The 6-year trends of MDA8 O_3 (solid blue line), meteorological adjusted O_3 (dashed blue line) and the meteorological impact (orange line) in the four cities during 2015–2020. Positive and negative meteorological impacts are shaded in red and green, respectively.

rainfall or diffusion effect (Ding et al., 2013; Ma et al., 2016; Zhang et al., 2013). By removing the short-term and seasonal components, the long-term components (Figures 6d, 6h, 6l, and 6p) showed a clear upward trend in XM and FZ. And the long-term trends of O_3 in LY and NP were relatively stable. These could be attributed to the difference of anthropogenic emissions among these cities. The concentrations of O_3 in all the four cities significantly increased during 2016–2018, which was consistent with the results mentioned in Section 3.1.

3.3.2. Quantifying the Contributions of Meteorological Factors

Using the method of meteorological adjustment described in Section 2.3, we obtained the meteorologically independent ozone series and evaluated their impacts on annual variations of O_3 (Figure 7). After the meteorological adjustment, the variable magnitude from 2015 to 2016 was higher than the original one, suggesting that the meteorological conditions reduced ambient O_3 concentrations. However, the opposite pattern from 2017 to 2020 was observed. These results were consisted with the weather typing findings that the frequencies of type A with high mean O_3 concentrations increased significantly during 2017–2018 (Figure 3b). For LY and NP, the variable magnitude was lower than that in XM and FZ. Totally, the changes of meteorological conditions resulted in varied O_3 concentrations by 16.4, 14.5, 2.6, and 4.3 μg cm^{-3} in XM, FZ, LY, and NP when the meteorological condition was most favorable for O_3 pollution during the study period, respectively, contributed to 20.46%, 16.5%, 8.1%, and 21.7% of the annual O_3 concentrations. These contributions in southeast coastal areas were higher than that in other megacities of China, such as the YRD (8.7%) (Gao et al., 2021), indicating that the O_3 concentrations are more sensitive to the changes of local meteorological conditions in our study area. However, the meteorological conditions become unfavorable to the increase of O_3 in FZ and LY from 2018 to 2019, leading to the reduction of O_3 up to 1.3 and 1.0 μg cm^{-3}, respectively, which is consistent with the O_3 decrease after 2018 discussed in Section 3.1. The sensitivity of long-term O_3 concentration to different meteorological factors varies in different cities (Figure S3 in Supporting Information S1). RH and BLH in XM were the key factors in long-term O_3 concentration variations. RH, SR, and LCC were observed to be important in the variation of the long-term ozone trend in FZ and LY. The O_3 trend in NP could be affected strongly by RH, SR, BLH, and TP.

The relative meteorological contributions are obtained, based on the different trends of O_3 series before and after meteorological adjustment (Table 1). The contribution in the four cities (58.6% in average) was significantly higher than in other urban areas such as Beijing-Tianjin-Hebei (31.8%) and YRD (27.8% and 29.8%). The meteorological contribution in this study was comparable to those of Houston (51.0%) and Portugal (59.0%), where the meteorological conditions was particularly important under stable anthropogenic emissions. In addition, the meteorological impacts on O_3 also show obvious differences in the four cities. The meteorological contribution in LY (66.1%) and NP (65.0%) were relatively high, due to the influence of lower anthropogenic emissions and more stable O_3 variabilities

Table 2
Pearson Coefficients Between MDA8 O_3 and Different Meteorological Factors in the Four Cities From 2015 to 2020

City	Factor	Correlation with MDA8 O_3 (R^2)			
		Short-term	Seasonal-term	Baseline	Long-term
XM	RH	−0.46***	−0.22***	−0.30***	−0.79***
	T_{max}	0.05**	0.34***	0.32***	0.75***
	U_{10}	0.15***	0.15***	−0.16***	−0.84***
	SR	−0.40***	−0.35***	0.37***	0.77***
	LCC	−0.40***	−0.26***	−0.39***	−0.87***
	TP	−0.23***	−0.13***	−0.19***	−0.77***
	BLH	0.06***	0.35***	0.34***	0.56***
	u	0.02	0.04	−0.01	−0.60***
	v	−0.06***	−0.22	−0.31***	−0.98***
	ξ	−0.24***	0.11	0.02	−0.54***
FZ	RH	−0.55***	−0.12***	−0.24***	−0.69***
	T_{max}	0.17***	0.55***	0.52***	0.60***
	U_{10}	−0.02	0.14***	0.06***	−0.89***
	V_{10}	0.08***	0.40***	0.31***	−0.83***
	SR	0.54***	0.70***	0.69***	0.88***
	LCC	−0.51***	−0.58***	−0.60***	−0.78***
	TP	−0.27***	0.21***	0.08***	−0.84***
	u	0.10***	0.52***	0.42***	−0.77***
	v	−0.03	0.36***	0.21***	−0.95***
	ξ	−0.31***	0.40***	0.25***	−0.70***
LY	RH	−0.66***	−0.33***	−0.36***	−0.66***
	T_{max}	0.35***	0.53***	0.52***	0.35***
	U_{10}	−0.06***	−0.01	−0.03	−0.60***
	V_{10}	−0.04*	0.05**	0.03	−0.65***
	SR	0.63***	0.62***	0.62***	0.71***
	LCC	−0.61***	−0.45***	−0.48***	−0.80***
	TP	−0.31***	0.02	−0.01	−0.65***
	BLH	0.36***	0.51***	0.51***	0.44***
	u	0.05**	0.23***	0.21***	−0.70***
	v	−0.02	0.01	−0.01	−0.47***
	ξ	−0.21***	0.30***	0.26***	−0.74***
NP	RH	−0.68***	−0.42***	−0.51***	−0.93***
	T_{max}	0.39***	0.62***	0.61***	0.80***
	SR	0.63***	0.71***	−0.61***	0.94***
	LCC	−0.60***	−0.61***	−0.64***	−0.87***
	TP	−0.35***	0.07***	0.25***	−0.98***
	BLH	0.35***	0.53***	0.37***	0.91***
	u	0.08***	0.44***	0.13***	−0.75***
	v	0.03	0.24***	0.31***	−0.91***
	ξ	−0.24***	0.44***	0.57***	−0.77***

than those in XM and FZ. Meanwhile, the meteorological contribution in XM (44.7%) was lower than that in FZ (58.4%), probably attributed to the impact of diffusion conditions. Other studies also found that the meteorological contribution will be larger with the reduction of emissions (Yin et al., 2019). These results indicated that the meteorological factors played more important role in these areas with relatively low anthropogenic activities emissions.

The baseline components, representing the sum of the seasonal and long-term components, were widely applied to discuss the impacts of key meteorological factors on O_3 variabilities (Ma et al., 2016; Yin et al., 2019; Yu et al., 2019). We furtherly analyzed the correlations between the baseline-components of MDA8 O_3 and meteorological factors (Table 2). The baseline components of SR were significantly correlated with MDA8 O_3 (0.37, 0.69, 0.62, and 0.61 in XM, FZ, LY, and NP, respectively, $p < 0.01$). LCC was proved to be important in all the four cities (−0.39, −0.60, −0.48, and −0.64 $p < 0.01$ in XM, FZ, LY, and NP, respectively), since clouds cover could regulate surface SR (Xia, 2010). Temperature has a good correlation with MDA8 O_3 in FZ (0.52, $p < 0.01$), LY (0.52, $p < 0.01$), and NP (0.61, $p < 0.01$), which were surrounded by mountains and had obvious temperature difference between day and night. Other studies also found that the baseline components of temperature had high correlations with the baseline components of MDA8 O_3 and the O_3 exceedance probabilities increased significantly in inland areas (Ma et al., 2016; Seo et al., 2014). Thus, these regions might suffer from more frequent O_3 pollution with the increasing temperature of global climate change. However, in subtropical humid zone, the baseline components of SR tended to present similar trends with the baseline components of MDA8 O_3 (Botlaguduru et al., 2018; Yin et al., 2019). This explains the lower O_3 concentration in summer in our study area, while the O_3 levels in northern inland cities tend to peak during summer (Ma et al., 2016).

To better understand the impact of climate change on O_3 trends, the long-term components of the meteorological factors and the correlation with long-term O_3 were calculated (Figures S4–S7 in Supporting Information S1 and Table 2). It was noted that all long-term meteorological factors showed a significant correlation with long-term O_3. Long-term O_3 was negatively related with RH, U_{10}, LCC, TP, u, v as well as with ξ, and positively related with T_{max}, BLH and SR. The significant decreasing trends of RH, LCC, and TP during 2016–2017 were observed, which provided favorable conditions to the formation of O_3, resulting in the increase of O_3 concentrations. From 2018 to 2019, the positive meteorological impacts on O_3 variations were found. Overall, RH, U_{10}, V_{10}, LCC, and TP decreased, and T_{max}, SR, BLH increased during the past 6 years. These trends of local meteorological factors demonstrated a relatively low humidity, high temperature, strong SR and less rainfall, which were beneficial to local photochemical reactions. It was noted that all the three circulation indexes were significantly negatively correlated with long-term O_3. The coefficients between long-term O_3 and v could reach 0.98 in XM, 0.95 in FZ and 0.91 in NP. V, defined as southerly flow component of the geostrophic surface wind, could present strength of southwest winds (weather type of WS) and the East Asian summer monsoon (Zhu et al., 2007). The decrease of v indicated a weakening of southwest winds and the East Asian summer monsoon, which could lead to an anomalous O_3 flux convergence and the increase of O_3 concentrations in southern China (Yang et al., 2022). In addition, the decrease of ξ during the past 6 years indicated the decrease of shear vorticity. This presented more type A and less type C, which were favorable to O_3 formation through photochemical reactions. These showed the impact of climate systems on O_3 variation.

4. Conclusions

The influence of synoptic patterns and meteorological factors on the long-term MDA8 O_3 variation in the coast of Southeast China from 2015 to 2020 were investigated. An increasing trend of O_3 concentrations in the cities (0.3–4.6 μg m^{-3} yr^{-1}) was found during the study period. The 23 synoptic patterns were clustered based on Lamb-Jenkinson weather typing approach, and it was proved that the changes of synoptic patterns strongly affected the variations of O_3 concentrations. Cyclone-related weather types and WS type were associated with low O_3 concentrations, while high O_3 levels tended to be found under type A. By considering both frequency and intensity variabilities of synoptic patterns, the reconstructed O_3 levels contributed to 46.0%–58.3% of the observed variability. The intensity of synoptic patterns was the dominant factor of inter-annual O_3 variability in most cities, and its frequency can play a more important role in the cities with lower emissions.

Significantly increasing trends of O_3 concentrations were found by separating the long-term components of O_3 series using KZ filter. After the meteorological adjustment, the relative meteorological contributions on O_3 trends in the cities in the coast area of southeast China ranged from 44.7% to 66.1%, which were much higher than in other regions of China. The results indicated the meteorological conditions was particularly important in the areas with less anthropogenic activities emissions. In addition, RH, BLH, SR and LCC were proved to play important roles in O_3 trends and variability. The higher temperature, lower RH, more SR, weakening southwest winds along with more anti-cyclone systems under climate change could increase surface O_3. This study demonstrated that meteorological conditions have significant impacts on the long-term O_3 variabilities in relatively clean areas, suggesting that O_3 pollution may still occur even the reduction of O_3 precursor emissions. Also, it is necessary for local governments to consider global climate change for mitigating O_3 pollution, especially the challenge from extreme weather conditions, for example, heat wave.

Data Availability Statement

A data set for this paper can be accessed at (Ji et al., 2022).

References

Botlaguduru, V. S. V., & Kommalapati, R. R. (2020). Meteorological detrending of long-term (2003-2017) ozone and precursor concentrations at three sites in the Houston Ship Channel Region. *Journal of the Air & Waste Management Association*, *70*(1), 93–107. https://doi.org/10.1080/10962247.2019.1694088

Botlaguduru, V. S. V., Kommalapati, R. R., & Huque, Z. (2018). Long-term meteorologically independent trend analysis of ozone air quality at an urban site in the greater Houston area. *Journal of the Air & Waste Management Association*, *68*(10), 1051–1064. https://doi.org/10.1080/10962247.2018.1466740

Chang, L., He, F., Tie, X., Xu, J., & Gao, W. (2021). Meteorology driving the highest ozone level occurred during mid-spring to early summer in Shanghai, China. *Science of the Total Environment*, *785*, 147253. https://doi.org/10.1016/j.scitotenv.2021.147253

Chen, Z., Liu, J., Cheng, X., Yang, M., & Wang, H. (2021). Positive and negative influences of typhoons on tropospheric ozone over southern China. *Atmospheric Chemistry and Physics*, *21*(22), 16911–16923. https://doi.org/10.5194/acp-21-16911-2021

Comrie, A. C., & Yarnal, B. (1992). Relationships between synoptic-scale atmospheric circulation and ozone concentrations in Metropolitan Pittsburgh, Pennsylvania. *Atmospheric Environment: Part B - Urban Atmosphere*, *26*(3), 301–312. https://doi.org/10.1016/0957-1272(92)90006-E

Ding, A., Wang, T., & Fu, C. (2013). Transport characteristics and origins of carbon monoxide and ozone in Hong Kong, South China. *Journal of Geophysical Research: Atmospheres*, *118*(16), 9475–9488. https://doi.org/10.1002/jgrd.50714

Dong, Y., Li, J., Guo, J., Jiang, Z., Chu, Y., Chang, L., et al. (2020). The impact of synoptic patterns on summertime ozone pollution in the North China Plain. *Science of the Total Environment*, *735*, 139559. https://doi.org/10.1016/j.scitotenv.2020.139559

Eskridge, R. E., Ku, J. Y., Rao, S. T., Porter, P. S., & Zurbenko, I. G. (1997). Separating different scales of motion in time series of meteorological variables. *Bulletin of the American Meteorological Society*, *78*(7), 1473–1483. https://doi.org/10.1175/1520-0477(1997)078<1473:SDSOMI>2.0.CO;2

Gao, D., Xie, M., Liu, J., Wang, T., Ma, C., Bai, H., et al. (2021). Ozone variability induced by synoptic weather patterns in warm seasons of 2014–2018 over the Yangtze River Delta region, China. *Atmospheric Chemistry and Physics*, *21*(8), 5847–5864. https://doi.org/10.5194/acp-21-5847-2021

Hegarty, J., Mao, H., & Talbot, R. (2007). Synoptic controls on summertime surface ozone in the northeastern United States. *Journal of Geophysical Research*, *112*(14306), 1–12. https://doi.org/10.1029/2006JD008170

Hertig, E., Schneider, A., Peters, A., von Scheidt, W., Kuch, B., & Meisinger, C. (2019). Association of ground-level ozone, meteorological factors and weather types with daily myocardial infarction frequencies in Augsburg, Southern Germany. *Atmospheric Environment*, *217*(116975), 1–9. https://doi.org/10.1016/j.atmosenv.2019.116975

Jenkinson, A., & Collison, F. (1977). *An initial climatology of gales over the North Sea*. Technical Report No. 18 (Vol. *62*). Meteorological Office.

Ji, X., Hong, y., Lin, Y., Chen, G., Liu, T., Xu, L., et al. (2022). Measurement report: Impacts of synoptic patterns and meteorological factors on distribution trends of ozone in Southeast China during 2015–2020 [Dataset]. Zenodo. https://doi.org/10.5281/zenodo.7091267

Jiang, Y., Xin, J., Wang, Y., Tang, G., Zhao, Y., Jia, D., et al. (2021). The thermodynamic structures of the planetary boundary layer dominated by synoptic circulations and the regular effect on air pollution in Beijing. *Atmospheric Chemistry and Physics*, *21*(8), 6111–6128. https://doi.org/10.5194/acp-21-6111-2021

Jing, P., O'Brien, T., Streets, D. G., & Patel, M. (2016). Relationship of ground-level ozone with synoptic weather conditions in Chicago. *Urban Climate*, *17*, 161–175. https://doi.org/10.1016/j.uclim.2016.08.002

Lamb, H. H. (1950). Types and spells of weather around the year in the British Isles: Annual trends, seasonal structure of the year, singularities. *Quarterly Journal of the Royal Meteorological Society*, *76*(330), 393–429. https://doi.org/10.1002/qj.49707633005

Liao, W., Wu, L., Zhou, S., Wang, X., & Chen, D. (2020). Impact of synoptic weather types on ground-level ozone concentrations in Guangzhou, China. *Asia-Pacific Journal of Atmospheric Sciences*, *57*(2), 169–180. https://doi.org/10.1007/s13143-020-00186-2

Liu, J., Wang, L., Li, M., Liao, Z., Sun, Y., Song, T., et al. (2019). Quantifying the impact of synoptic circulation patterns on ozone variability in northern China from April to October 2013–2017. *Atmospheric Chemistry and Physics*, *19*(23), 14477–14492. https://doi.org/10.5194/acp-19-14477-2019

Lu, X., Hong, J., Zhang, L., Cooper, O. R., Schultz, M. G., Xu, X., et al. (2018). Severe surface ozone pollution in China: A global perspective. *Environmental Science and Technology Letters*, *5*(8), 487–494. https://doi.org/10.1021/acs.estlett.8b00366

Lu, X., Zhang, L., Chen, Y., Zhou, M., Zheng, B., Li, K., et al. (2019). Exploring 2016–2017 surface ozone pollution over China: Source contributions and meteorological influences. *Atmospheric Chemistry and Physics*, *19*(12), 8339–8361. https://doi.org/10.5194/acp-19-8339-2019

Ma, Z., Xu, J., Quan, W., Zhang, Z., Lin, W., & Xu, X. (2016). Significant increase of surface ozone at a rural site, north of eastern China. *Atmospheric Chemistry and Physics*, *16*(6), 3969–3977. https://doi.org/10.5194/acp-16-3969-2016

Milanchus, M. L., Rao, S. T., & Zurbenko, I. G. (1998). Evaluating the effectiveness of ozone management efforts in the presence of meteorological variability. *Journal of the Air & Waste Management Association*, *48*(3), 201–215. https://doi.org/10.1080/10473289.1998.10463673

Monks, P. S., Granier, C., Fuzzi, S., Stohl, A., Williams, M. L., Akimoto, H., et al. (2009). Atmospheric composition change—Global and regional air quality. *Atmospheric Environment*, *43*(33), 5268–5350. https://doi.org/10.1016/j.atmosenv.2009.08.021

Mousavinezhad, S., Choi, Y., Pouyaei, A., Ghahremanloo, M., & Nelson, D. L. (2021). A comprehensive investigation of surface ozone pollution in China, 2015–2019: Separating the contributions from meteorology and precursor emissions. *Atmospheric Research*, *257*, 105599. https://doi.org/10.1016/j.atmosres.2021.105599

Rao, S. T., Zurbenko, I., Neagu, R., Porter, P., Ku, M., & Henry, R. (1997). Space and time scales in ambient ozone data. *Bulletin of the American Meteorological Society*, *78*(10), 2153–2166. https://doi.org/10.1175/1520-0477(1997)078<2153:SATSIA>2.0.CO;2

Rao, S. T., & Zurbenko, I. G. (1994). Detecting and tracking changes in ozone air quality. *Air & Waste*, *44*(9), 1089–1092. https://doi.org/10.1080/10473289.1994.10467303

Sá, E., Tchepel, O., Carvalho, A., & Borrego, C. (2015). Meteorological driven changes on air quality over Portugal: A KZ filter application. *Atmospheric Pollution Research*, *6*(6), 979–989. https://doi.org/10.1016/j.apr.2015.05.003

Santurtún, A., González-Hidalgo, J. C., Sanchez-Lorenzo, A., & Zarrabeitia, M. T. (2015). Surface ozone concentration trends and its relationship with weather types in Spain (2001–2010). *Atmospheric Environment*, *101*, 10–22. https://doi.org/10.1016/j.atmosenv.2014.11.005

Schnell, J. L., Prather, M. J., Josse, B., Naik, V., Horowitz, L. W., Zeng, G., et al. (2016). Effect of climate change on surface ozone over North America, Europe, and East Asia. *Geophysical Research Letters*, *43*(7), 3509–3518. https://doi.org/10.1002/2016gl068060

Seo, J., Youn, D., Kim, J. Y., & Lee, H. (2014). Extensive spatiotemporal analyses of surface ozone and related meteorological variables in South Korea for the period 1999–2010. *Atmospheric Chemistry and Physics*, *14*(12), 6395–6415. https://doi.org/10.5194/acp-14-6395-2014

Shu, L., Wang, T., Han, H., Xie, M., Chen, P., Li, M., & Wu, H. (2020). Summertime ozone pollution in the Yangtze River Delta of eastern China during 2013-2017: Synoptic impacts and source apportionment. *Environmental Pollution*, *257*, 113631. https://doi.org/10.1016/j.envpol.2019.113631

Silver, B., Reddington, C. L., Arnold, S. R., & Spracklen, D. V. (2018). Substantial changes in air pollution across China during 2015–2017. *Environmental Research Letters*, *13*(11), 114012. https://doi.org/10.1088/1748-9326/aae718

Trigo, R. M., & DaCamara, C. C. (2000). Circulation weather types and their influence on the precipitation regime in Portugal. *International Journal of Climatology*, *20*(13), 1559–1581. https://doi.org/10.1002/1097-0088(20001115)20:13<1559::AID-JOC555>3.0.CO;2-5

Wang, N., Zhu, L., Yang, H., & Han, L. (2017). Classification of synoptic circulation patterns for fog in the Urumqi Airport. *Atmospheric and Climate Sciences*, *07*(03), 352–366. https://doi.org/10.4236/acs.2017.73026

Wang, T., Xue, L., Feng, Z., Dai, J., Zhang, Y., & Tan, Y. (2022). Ground-level ozone pollution in China: A synthesis of recent findings on influencing factors and impacts. *Environmental Research Letters*, *17*(6), 063003. https://doi.org/10.1088/1748-9326/ac69fe

Wu, P., Ding, Y., & Liu, Y. (2017). Atmospheric circulation and dynamic mechanism for persistent haze events in the Beijing–Tianjin–Hebei region. *Advances in Atmospheric Sciences*, *34*(4), 429–440. https://doi.org/10.1007/s00376-016-6158-z

Xia, X. (2010). Spatiotemporal changes in sunshine duration and cloud amount as well as their relationship in China during 1954–2005. *Journal of Geophysical Research*, *115*, D00K06. https://doi.org/10.1029/2009jd012879

Yan, Y., Zhou, Y., Kong, S., Lin, J., Wu, J., Zheng, H., et al. (2021). Effectiveness of emission control in reducing $PM_{2.5}$ pollution in central China during winter haze episodes under various potential synoptic controls. *Atmospheric Chemistry and Physics*, *21*(4), 3143–3162. https://doi.org/10.5194/acp-21-3143-2021

Yang, Y., Li, M., Wang, H., Li, H., Wang, P., Li, K., et al. (2022). ENSO modulation of summertime tropospheric ozone over China. *Environmental Research Letters*, *17*(3), 034020. https://doi.org/10.1088/1748-9326/ac54cd

Yin, C., Deng, X., Zou, Y., Solmon, F., Li, F., & Deng, T. (2019). Trend analysis of surface ozone at suburban Guangzhou, China. *Science of the Total Environment*, *695*, 133880. https://doi.org/10.1016/j.scitotenv.2019.133880

Yu, Y., Wang, Z., He, T., Meng, X., Xie, S., & Yu, H. (2019). Driving factors of the significant increase in surface ozone in the Yangtze River Delta, China, during 2013–2017. *Atmospheric Pollution Research*, *10*(4), 1357–1364. https://doi.org/10.1016/j.apr.2019.03.010

Zhan, C., Xie, M., Huang, C., Liu, J., Wang, T., Xu, M., et al. (2020). Ozone affected by a succession of four landfall typhoons in the Yangtze River Delta, China: Major processes and health impacts. *Atmospheric Chemistry and Physics*, *20*(22), 13781–13799. https://doi.org/10.5194/acp-20-13781-2020

Zhang, J., Gao, Y., Leung, L. R., Luo, K., Wang, M., Zhang, Y., et al. (2022). Isolating the modulation of mean warming and higher-order temperature changes on ozone in a changing climate over the contiguous United States. *Environmental Research Letters*, *17*(9), 094005. https://doi.org/10.1088/1748-9326/ac8695

Zhang, J., Gao, Y., Luo, K., Leung, L. R., Zhang, Y., Wang, K., & Fan, J. (2018). Impacts of compound extreme weather events on ozone in the present and future. *Atmospheric Chemistry and Physics*, *18*(13), 9861–9877. https://doi.org/10.5194/acp-18-9861-2018

Zhang, X., Wu, Z., He, Z., Zhong, X., Bi, F., Li, Y., et al. (2022). Spatiotemporal patterns and ozone sensitivity of gaseous carbonyls at eleven urban sites in southeastern China. *Science of the Total Environment*, *824*, 153719. https://doi.org/10.1016/j.scitotenv.2022.153719

Zhang, Y., Mao, H., Ding, A., Zhou, D., & Fu, C. (2013). Impact of synoptic weather patterns on spatio-temporal variation in surface O_3 levels in Hong Kong during 1999–2011. *Atmospheric Environment*, *73*, 41–50. https://doi.org/10.1016/j.atmosenv.2013.02.047

Zhu, Y., Chen, D., Li, W., & Zhang, P. (2007). Lamb-Jenkinson circulation type classification system and its application in China. *Journal of Nanjing Institute of Meteorology*, *30*(3). https://doi.org/10.13878/j.cnki.dqkxxb.2007.03.001